Improving depth resolution of diffuse optical tomography with an exponential adjustment method based on maximum singular value of layered sensitivity

Haijing Niu (牛海晶)[1], Ping Guo (郭 平)[1,2], Xiaodong Song (宋晓东)[3], and Tianzi Jiang (蒋田仔)[4]

[1]*Image Processing and Pattern Recognition Laboratory, Beijing Normal University, Beijing 100875*

[2]*School of Computer Science and Technology, Beijing Institute of Technology, Beijing 100081*

[3]*School of Aerospace Science and Engineering, Beijing Institute of Technology, Beijing 100081*

[4]*National Laboratory of Pattern Recognition, Institute of Automation, Chinese Academy of Sciences, Beijing 100081*

Received September 16, 2008

The sensitivity of diffuse optical tomography (DOT) imaging exponentially decreases with the increase of photon penetration depth, which leads to a poor depth resolution for DOT. In this letter, an exponential adjustment method (EAM) based on maximum singular value of layered sensitivity is proposed. Optimal depth resolution can be achieved by compensating the reduced sensitivity in the deep medium. Simulations are performed using a semi-infinite model and the simulation results show that the EAM method can substantially improve the depth resolution of deeply embedded objects in the medium. Consequently, the image quality and the reconstruction accuracy for these objects have been largely improved.

OCIS codes: 170.6960, 170.3010, 170.3880.

doi: 10.3788/COL20080612.0886.

Diffuse optical tomography (DOT) is an emerging technology that can reconstruct the optical properties of internal biological tissue from the region under investigation[1]. It is noninvasive and portable, and can produce real-time images of clinically relevant parameters[2]. When photon propagates in tissue, the sensitivity of diffuse-light measurements drops off quickly with penetration depth. This leads to poor depth resolution in deep tissue[3]. Because of this drawback, many important biological investigations such as breast tumor or cortex activations of the brain have been limited since those changes generally happen beneath several millimeters of this investigated tissue.

Boas *et al.* showed that increasing the number of overlapping measurements or enlarging source-detector separation can achieve improved depth resolution for near-infrared imaging[4]. Also, hybrid image reconstruction methods such as near-infrared DOT combined with prior magnetic resonance imaging (MRI) structural information have also been proved to be able to overcome the depth limitation for DOT imaging in certain extent[5]. In addition, both the spatial varying regularization (SVR) method[6] and the layered-based sigmoid adjustment (LSA) method[7] played an important role in improving depth resolution of DOT imaging. In this letter, we present an exponential adjustment method (EAM) based on maximum singular value of layered sensitivity, which can improve depth resolution of the DOT imaging by compensating the decreased sensitivity in the deep medium. This novel method is validated by simulations of semi-infinite medium with the depth of 60 mm, in which the object is individually located in different depths.

The photon propagation in highly scattering medium obeys diffusion equation[8]. When only absorption changes are considered, the analytic solution of the diffusion equation can be obtained by[9]

$$\Delta \mathrm{OD} = -\ln\left(\frac{\Phi_{\mathrm{pert}}}{\Phi_0}\right) = \int \Delta\mu_{\mathrm{a}}(r) L(r) \mathrm{d}r, \qquad (1)$$

where ΔOD is the change in optical density, Φ_0 is the simulated photon fluence in a semi-infinite medium, and Φ_{pert} is the simulated photon fluence with the absorbers included. The second part of Eq. (1) is known as the modified Beer-Lambert law, in which $\Delta\mu_{\mathrm{a}}(r)$ is the change in absorption coefficient and $L(r)$ is the effective average path length of the photons.

Equation (1) is generalized for a set of discrete voxels and written as $\mathbf{y} = \mathbf{A}\mathbf{x}$, where $\mathbf{y}$ is the vector of measured changes in optical density from all the measurements, $\mathbf{x}$ is the vector of the unknown change in absorption coefficient in all of the voxels, and the matrix $\mathbf{A}$ describes the sensitivity that each measurement divides the change in absorption within each voxel in the medium. The sum of matrix $\mathbf{A}$ by rows indicates the overall sensitivity of each voxel from all measurements, and it displays an exponential decrease distribution in an increased depth dimension[7].

To compensate the dramatic decrease in sensitivity, an exponential diagonal matrix $\mathbf{M}$ based on layered maximum singular values is multiplied on the forward matrix $\mathbf{A}$. The adjusted forward matrix $\mathbf{A}^{\#}$ and the weight matrix $\mathbf{M}$ are written as

$$\mathbf{A}^{\#} = \mathbf{A}\mathbf{M},$$

$$\mathbf{M} = \begin{bmatrix} M_L & & & & & & \\ & \ddots & & & & & \\ & & M_L & & & & \\ & & & \ddots & & & \\ & & & & M_1 & & \\ & & & & & \ddots & \\ & & & & & & M_1 \end{bmatrix}^{\gamma}, \qquad (2)$$

where γ is termed as adjustment exponent and it is empirically determined in the range of 0 to 3; M_1, M_2, $\cdots$, M_L are the maximum singular values for the forward matrix from the first top layer to the bottom Lth layer when assuming that the reconstructed image contains L layers. These layered singular values are exponentially distributed[9], which guarantees that these elements in weight matrix $\mathbf{M}$ take exponential configuration as γ changed.

In the weight matrix $\mathbf{M}$, $(M_L)^\gamma$ is the adjustment coefficient for the first layer, and $(M_{L-1})^\gamma$ for the second layer, and so on. $(M_1)^\gamma$ is the adjustment coefficient for the Lth layer (i.e., bottom layers). That means these elements are inversely used to adjust the sensitivity distribution. Thus, the new reconstruction equation for EAM is given by $\mathbf{x} = \mathbf{M}\mathbf{A}^{\mathrm{T}}(\mathbf{A}\mathbf{M}^2\mathbf{A}^{\mathrm{T}} + \lambda\sigma_{\max}\mathbf{I})^{-1}\mathbf{y}$.

Changing the value of γ will vary the dynamic range of the weight matrix $\mathbf{M}$, therefore it will ultimately change the sensitivity distribution between deep and superficial layers. For example, with the increase of adjustment exponent γ, $\mathbf{M}$ will obtain a large dynamic range, thus the elements for deep layers can acquire a larger adjustment coefficient compared with those in superficial layers. On the contrary, lessening the adjustment exponent, the dynamic range for the weight matrix will decrease; correspondingly, the elements for deep layers will obtain a small adjustment coefficient. Figure 1 shows the sensitivity distributions in x-z plane when γ is changed from 0 to 3 with an increment of 0.5 and the corresponding sensitivity curves in depth dimension.

It can be seen from Fig. 1(a) that the larger sensitivity occurs in superficial layers when γ is equal to zero, which agrees with the general investigation, i.e., photon sensitivity exponentially decreases with penetration depth[3]. With the increase of γ from 0 to 3, the sensitivity of superficial layers is decreased and larger sensitivity biases towards the deep layers, as shown in Figs. 1(b)—(g), which would be anticipated to bring about improved depth resolution for deep object imaging.

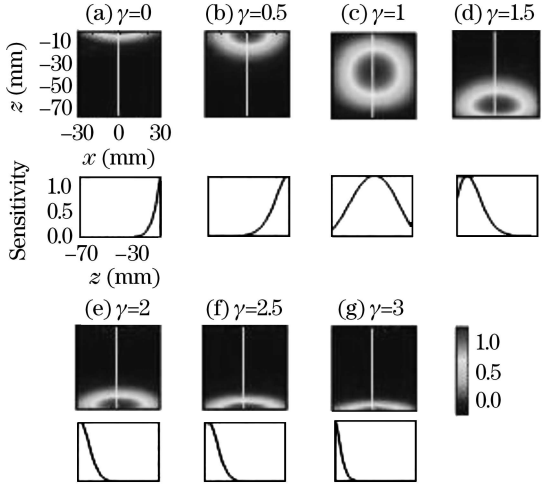

Fig. 1. Sensitivity profiles within x-z slice with varying adjustment exponent γ from 0 to 3 at an increment of 0.5 and their corresponding sensitivity profiles with $x = 0$ in the x-z slice. The depth for imaging fields is 60 mm from −10 to −70 mm. The scale in the sensitivity is normalized.

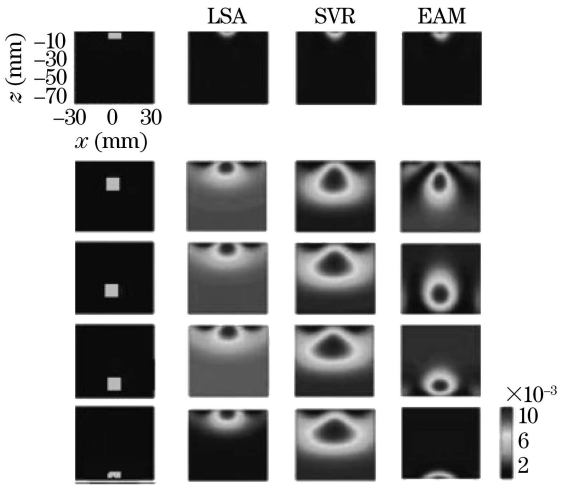

Fig. 2. The first column shows real images with object located in depths −10, −30, −50, −60, and −70 mm from up to down and their reconstructed images with LSA, SVR, and EAM methods are shown in the second, third, and fourth columns, respectively.

To illustrate the validation of this sensitivity adjustment, we performed simulations based on a semi-infinite medium. The imaging field area for this medium was set to be 60×60 (mm) in x-y plane and the depth in z direction was 60 mm (from −10 to −70 mm). The background absorption and reduced scattering coefficients for the medium were 0.01 and 1.0 mm^{-1}, respectively. Absorption inclusions were located separately in depths −10, −20, −40, −60, and −70 mm, as shown in Fig. 2 (the first column). The absorption coefficient and radius for these inclusions were 0.03 mm^{-1} and 3 mm, respectively. A hexagonal configuration of 7 sources and 24 detectors was arranged on the surface of the imaging region, which produced 168 measurements[11]. Random Gauss-distributed noise was added to the simulated data to achieve measurements with approximate signal-to-noise ratio (SNR) of 1000.

The reconstructed images for the EAM method are shown in Fig. 2 (the fourth column). The adjustment exponent for EAM images were empirically chosen as 0, 1.1, 1.5, 1.8, and 3, respectively. For comparison, the SVR[6] and LSA[7] techniques were also implemented to conduct reconstruction under the same imaging conditions, and the reconstruction equations for these methods were respectively given by $\mathbf{x} = \mathbf{D}\cdot\mathbf{D}\mathbf{A}^{\mathrm{T}}(\mathbf{A}\mathbf{D}^2\mathbf{A}^{\mathrm{T}} + \lambda\mathbf{I})^{-1}\mathbf{y}$ and $\mathbf{x} = \mathbf{D}\mathbf{A}^{\mathrm{T}}(\mathbf{A}\mathbf{D}^2\mathbf{A}^{\mathrm{T}} + \lambda\mathbf{I})^{-1}\mathbf{y}$, in which $\mathbf{D}$ was a diagonal matrix generated by LSA method and $\mathbf{A}$ was the initial forward matrix. The SVR and LSA images are respectively shown in the second and third columns of Fig. 2. The L-curve method[12] was applied to choose optimal regularization value for each method. The voxel size in these reconstructed images was 1 mm^{-3}.

We utilized two criteria to evaluate the quality of reconstructed image: contrast-to-noise ratio (CNR)[13] and positional error (PE). CNR indicates whether an object can be clearly detected from the background of reconstructed images, while PE is the distance between centers of the real object and the detected object. Larger CNR values and smaller PE values are considered as higher image quality. The evaluations for these reconstructions

Table 1. CNR and PE Values for the Reconstructed Images Shown in Fig. 2

Depth	LSA		SVR		EAM	
(mm)	CNR	PE (mm)	CNR	PE (mm)	CNR	PE (mm)
−10	32.65	0.46	26.69	0.21	43.01	0.12
−30	1.90	12.77	4.78	1.34	13.54	0.31
−50	0.35	31.69	0.32	20.15	10.06	0.28
−60	0.63	41.16	0.20	32.15	10.39	0.45
−70	0.73	49.81	0.16	38.73	18.08	0.13

are shown in Table 1.

It is found that all these three methods can accurately reconstruct the superficial objects located in the depth of −10 mm. However, with the increase of object depth, the objects reconstructed with LSA and SVR cannot accurately be recognized from the background, in response, the smaller CNR and larger PE for these reconstructions from depths −30 to −70 mm are shown in Table 1. These indicate that the LSA and SVR methods cannot effectively locate these deep objects in imaging fields. Compared with LSA and SVR, the EAM approach can achieve satisfactory image quality and optimal reconstruction accuracy for these objects embedded in deep medium. Correspondingly, the high CNR and small PE values have been acquired for their images, as shown in Table 1, which demonstrates that the scheme is a really effective approach for improving the depth resolution of DOT imaging.

It is necessary to point out that the adjustment exponent γ in EAM is an important parameter for obtaining these optimal reconstructions. In this letter, this parameter is determined empirically and in our future study it is anticipated to be adaptively or automatically chosen for achieving optimal reconstructions.

In summary, we have presented the EAM method and investigated its validation in improving the depth resolution of DOT imaging through simulations based on a semi-infinite model with objects located in depths from −10 to −70 mm. Simultaneously, we have made a comparison among our proposed EAM method and the SVR and LSA techniques, and the results clearly illustrate that our EAM can improve the depth resolution of deep object imaging. These results also demonstrate that the sensitivity compensation technique is effective. It is worth pointing out that the deep objects can be accurately reconstructed without utilizing anomaly information from MRI or X-ray. A series of experiments is required for the validation of the methodology in practical applications.

This work was supported by the National Natural Science Foundation of China (No. 60675011 and 30425004), the National "973" Program of China (No. 2003CB716100), and the National "863" Program of China (No. 2006AA01Z132). T. Jiang is the author to whom the correspondence should be addressed, his e-mail address is jiangtz@nlpr.ia.ac.cn.

References

1. H. Niu, P. Guo, L. Ji, Q. Zhao, and T. Jiang, Opt. Express **16,** 12423 (2008).
2. F. Gao, Y. Xue, H. Zhao, T. Kusaka, M. Ueno, and Y. Yamada, Chin. Opt. Lett. **5,** 472 (2007).
3. J. P. Culvder, A. M. Siegel, J. Siegel, J. J. Stott, and D. A. Boas, Opt. Lett. **28,** 2061 (2003).
4. D. A. Boas and A. M. Dale, Appl. Opt. **44,** 1957 (2005).
5. R. L. Barbour, H. L. Graber, J. Chang, S.-L. S. Barbour, P. C. Koo, and R. Aronson, IEEE Comput. Sci. Eng. **2,** 63 (1995).
6. B. W. Pogue, T. O. McBride, J. Prewitt, U. L. Österberg, and K. D. Paulsen, Appl. Opt. **38,** 2950 (1999).
7. Q. Zhao, L. Ji, and T. Jiang, Opt. Express **15,** 4018 (2007).
8. K. D. Paulsen and H. Jiang, Med. Phys. **22,** 691 (1995).
9. D. T. Delpy, M. Cope, P. van der Zee, S. Arridge, S. Wray, and J. Wyatt, Phys. Med. Biol. **33,** 1433 (1988).
10. H.-J. Niu, P. Guo, and T.-Z. Jiang, Lecture Notes in Computer Science **5226,** 514 (2008).
11. Q. Zhao, L. Ji, and T. Jiang, J. Biomed. Opt. **11,** 064019 (2006).
12. P. C. Hansen and D. P. O'Leary, SIAM J. Sci. Comput. **14,** 1487 (1993).
13. X. Song, B. W. Pogue, S. Jiang, M. M. Doyley, H. Dehghani, T. D. Tosteson, and K. D. Paulsen, Appl. Opt. **43,** 1053 (2004).